The current issue and full text archive of this journal is available on Emerald Insight at:
https://www.emerald.com/insight/1756-8692.htm

Received 6 June 2020
Revised 11 August 2020
10 November 2020
18 November 2020
Accepted 10 December 2020

Extreme climate response to marine cloud brightening in the arid Sahara-Sahel-Arabian Peninsula zone

Yuanzhuo Zhu
Climate Modeling Laboratory, School of Mathematics, Shandong University, Jinan, China

Zhihua Zhang
Climate Modeling Laboratory, School of Mathematics, Shandong University, Jinan, China and MOE Key Laboratory of Environmental Change and Natural Disaster, Beijing Normal University, China, and

M. James C. Crabbe
Wolfson College, Oxford University, Oxford, UK; Institute of Biomedical and Environmental Science and Technology, University of Bedfordshire, Luton, UK and School of Life Sciences, Shanxi University, Taiyuan, China

Abstract

Purpose – Climatic extreme events are predicted to occur more frequently and intensely and will significantly threat the living of residents in arid and semi-arid regions. Therefore, this study aims to assess climatic extremes' response to the emerging climate change mitigation strategy using a marine cloud brightening (MCB) scheme.

Design/methodology/approach – Based on Hadley Centre Global Environmental Model version 2-Earth System model simulations of a MCB scheme, this study used six climatic extreme indices [i.e. the hottest days (TXx), the coolest nights (TNn), the warm spell duration (WSDI), the cold spell duration (CSDI), the consecutive dry days (CDD) and wettest consecutive five days (RX5day)] to analyze spatiotemporal evolution of climate extreme events in the arid Sahara-Sahel-Arabian Peninsula Zone with and without MCB implementation.

Findings – Compared with a Representative Concentration Pathways 4.5 scenario, from 2030 to 2059, implementation of MCB is predicted to decrease the mean annual TXx and TNn indices by 0.4–1.7 and 0.3–2.1°C, respectively, for most of the Sahara-Sahel-Arabian Peninsula zone. It would also shorten the mean annual WSDI index by 118–183 days and the mean annual CSDI index by only 1–3 days, especially in the southern Sahara-Sahel-Arabian Peninsula zone. In terms of extreme precipitation, MCB could also decrease the mean annual CDD index by 5–25 days in the whole Sahara and Sahel belt and increase the mean annual RX5day index by approximately 10 mm in the east part of the Sahel belt during 2030–2059.

© Yuanzhuo Zhu, Zhihua Zhang and M. James C. Crabbe. Published by Emerald Publishing Limited. This article is published under the Creative Commons Attribution (CC BY 4.0) licence. Anyone may reproduce, distribute, translate and create derivative works of this article (for both commercial and non-commercial purposes), subject to full attribution to the original publication and authors. The full terms of this licence may be seen at http://creativecommons.org/licences/by/4.0/legalcode

The authors are very grateful to the referees for their valuable suggestions.

This research was partially supported by the Second Tibetan Plateau Scientific Expedition and Research No 2019QZKK0906; European Commission Horizon2020 Flagship Project "ePIcenter"; Taishan Distinguished Professorship Fund.

International Journal of Climate Change Strategies and Management
Vol. 13 No. 3, 2021
pp. 250-265
Emerald Publishing Limited
1756-8692
DOI 10.1108/IJCCSM-06-2020-0051

Downloaded from http://ftp.nowpublishers.com/ijccsm/article-pdf/13/3/250/1144612/ijccsm-06-2020-0051.pdf by guest on 24 May 2026

Originality/value – The results provide the first insights into the impacts of MCB on extreme climate in the arid Sahara-Sahel-Arabian Peninsula zone.

Keywords Climatic extremes, Marine cloud brightening scheme, Sahara-Sahel-Arabian Peninsula zone, Spatiotemporal evolution

Paper type Research paper

1. Introduction

Arid and semi-arid regions have experienced the most significant temperature increases in the past 100 years, which have contributed 44% to past land warming (Huang *et al.*, 2012). The Sahara-Sahel-Arabian Peninsula zone, located at a crossroads of global climate patterns, is characterized by a hot and arid climate, so this zone is extremely sensitive to climate change. During the past 30 years, the western part of the Sahara-Sahel-Arabian Peninsula zone has had a tendency towards humid conditions, whereas the eastern part has had an increasing drought trend (Donat *et al.*, 2014). At the same time, cold temperature extremes decreased and warm temperature extremes increased over the Arabian Peninsula during 1986–2008 (AlSarmi and Washington, 2014); especially, in Riyadh city, Saudi Arabia, extremes of warm night and warm days were increased by 10% and 5%, respectively, per decade during 1986–2014 (Tarawneh and Faraj, 2020). Based on simulations of the UK Hadley Center's climate model, the rainfall in North Africa, Egypt, Saudi Arabia, Iran, Syria, Jordan and Israel by 2050s is expected to be 20%–25% lower than the present values, accompanied by a temperature increase of about 2–2.75°C (Ragab and Prudhomme, 2002). By analysis projections from the Coupled Model Intercomparison Project Phase 5, the summer maximum temperature for most cities in the Arabian Peninsula is likely to increase continuously at the rate of about 0.2°C per decade under Representative Concentration Pathways 4.5 (RCP4.5) during 2020–2099, which is significant at the 99% confidence level (Almazroui, 2020).

Increasing carbon emissions lead to both past and future climate change in the Sahara-Sahel-Arabian Peninsula zone. At the same time, international negotiations on reduction of carbon emissions have largely failed, e.g. The Paris climate agreement did not reach a mandatory emission reduction agreement. Therefore, a marine cloud brightening (MCB) scheme has been proposed to cool the climate by increasing the cloud albedo to reflect a small amount of solar radiation back into space. The core of this scheme is to add suitable cloud condensation nuclei, for instance, sea salt, into the marine boundary layer, which can enhance the cloud droplet number concentration (CDNC) and reduce the droplet sizes and finally lead to an increase of the cloud albedo. Modeling of a MCB scheme has revealed that it could work well in climate cooling. However, MCB demonstrates significant regional differences (Zhang and Huisingh, 2015): some countries and regions would gain considerably, whereas others might be faced with a worse set of circumstances than would be the case without MCB. At present, research on impacts and responses of MCB is in its early phase, mainly on the global scale and with average climate parameters: Jones *et al.* (2009) found that a significant drying would occur in the Amazon basin; Bala *et al.* (2011) found that global-mean precipitation and evaporation would decrease by about 1.3% but runoff over land increase by 7.5%; Stjern *et al.* (2018) predicted that with MCB the global average temperature during 2020–2060 would decrease −0.18 to −1.19°C relative to an RCP4.5 scenario, with particularly strong cooling over low-latitude zones. Our results provide the first insight in impacts of MCB on extreme climate in the arid Sahara-Sahel-Arabian Peninsula zone.

Present and future climate change always results in increasing climate variability, especially in terms of climatic extreme events. At the same time, climatic extreme events will have severe impacts on ecosystems, agriculture and human society in arid and semi-arid

Downloaded from http://ftp.nowpublishers.com/ijccsm/article-pdf/13/3/250/1144612/ijccsm-06-2020-0051.pdf by guest on 24 May 2026

regions where spatial and temporal distributions of water resources are directly impacted (Zhang *et al.*, 2009). In the arid and semi-arid Sahara-Sahel-Arabian Peninsula zone, severe hot waves are already intolerable for human beings in many parts and can produce significant agricultural damage and power outages. Thus, it is of great value to study the extreme climate response to MCB in the arid and semi-arid Sahara-Sahel-Arabian Peninsula zone. In this study, we explored the changing characteristics of extreme temperature and precipitation events with and without the implementation of a MCB scheme in the Sahara-Sahel-Arabian Peninsula zone.

2. Data and methods

2.1 Study area

The study area was chosen as the largest arid and semi-arid region in the world, i.e. the Sahara-Sahel-Arabian Peninsula zone. The Sahara is located in northern Africa, starting from the coast of the Atlantic Ocean, bordering the Atlas Mountains and the Mediterranean Sea in the north and connecting with the Sahel in the south and Arabian Peninsula through Sinai Peninsula. The Sahara, covering 32% of the total area of Africa, is extremely arid. Geographically, the Sahara can be divided into three parts: Western Sahara, Central Plateau (Algarh Plateau, Al Plateau and Tibezian Plateau) and Eastern Deserts (Tenere Desert and Libyan desert). Its climate is characterized by high temperatures, extremely low and erratic rainfall, extremely high sunshine duration and extremely high evaporation (Griffiths, 2013). The Sahel, lying between the Sahara to the north and the wooded Sudanian Savanna to the south, is a transitional eco-region characterized by semi-arid grasslands, savannas, steppes and thorn shrublands. The Sahel has a tropical, hot steppe climate with an unvarying temperature. The Arabian Peninsula, located in the east of the Sahara, is the largest peninsula in the world. It is dominated by deserts, except for mountain ranges in the southwest, which receive significantly more rainfall.

2.2 Hadley Centre Global Environmental Model version 2-Earth System model

The Hadley Centre Global Environmental Model version 2-Earth System (HadGEM2-ES) has been widely used to simulate and predict evolution of global climate systems (Jones *et al.*, 2011; Caesar *et al.*, 2013; Moss *et al.*, 2010; Brands *et al.*, 2013; Zhang and Huisingh, 2015; Almagro *et al.*, 2020). The HadGEM2-ES model is a coupled AOGCM with atmospheric resolution 1.875° × 1.25° and ocean resolution of 1° (increasing to 1/3° at the equator). As biogeochemical feedback schemes are introduced in the HadGEM2-ES model to represent interactive land/ocean carbon cycles and dynamic vegetation as well as interactive tropospheric chemistry (Jones *et al.*, 2011; Caesar *et al.*, 2013; Moss *et al.*, 2010, Johns *et al.*, 2006), the HadGEM2-ES model can not only simulate a realistic state of climate, vegetation and ocean biology with no need for artificial correction terms but also predict the true uncertainty of the future evolution of climate (Collins *et al.*, 2011). Moreover, Haywood *et al.* (2014) indicated that HadGEM2-ES has the second highest equilibrium climate sensitivity in 15 known climate models. Through detailed comparison with satellite and reanalysis data and *in situ* measurements, the HadGEM2-ES model was proved to have good simulation of temperature and precipitation patterns over Africa (Dike *et al.*, 2015). Brands *et al.* (2013) showed that the HadGEM2-ES outperforms CanESM2, CNRM-CM5, IPSL-CM5-MR, MICRO-ESM and NorESM1-M in the CORDEX Africa (i.e. Africa + Middle East). Shiru *et al.* (2020) used symmetrical uncertainty, gain ratio and entropy gain to rank the projection performance of climate models and indicated that the HadGEM2-ES model is the second-best model among 20 known climate models to simulate climate of Nigeria in Africa. Based on all above excellent performance, we use the prediction by HadGEM2-ES model to analyze spatiotemporal evolution of climate extreme events in the Arid Sahara-Sahel-Arabian Peninsula Zone with and without MCB implementation.

Downloaded from http://ftp.nowpublishers.com/ijccsm/article-pdf/13/3/250/1144612/ijccsm-06-2020-0051.pdf by guest on 24 May 2026

2.3 Modeling of marine cloud brightening scheme

Modeling of a MCB scheme is included in the Geoengineering Model Intercomparison Project (GeoMIP), where the future scenario is assumed to follow RCP4.5 (Kravitz *et al.*, 2013a, 2013b). RCP4.5 is the middle-of-the-road scenario which assumes continued greenhouse gas emission increases from today's levels, followed by a decrease from year 2040 and stabilization by year 2100, at which time the anthropogenic radiative forcing amounts to 4.5 W m^{-2} above preindustrial levels (Meinshausen *et al.*, 2011; Taylor *et al.*, 2012). The modeling of a MCB scheme was assumed to be implemented through a 50% increase in the CDNC of marine clouds below 680 hPa during 2020–2069. As this modeling experiment is included in the fourth experimental set in GeoMIP, it is also so-called the G4cdnc experiment. The HadGEM2-ES model was used to run a G4cdnc experiment (Kravitz *et al.*, 2013a, 2013b). To avoid initial and termination effects, we only analyzed the predicted temperature and precipitation data during the period 2030–2059. To make further comparisons with historical climates, historical simulations of HadGEM2-ES for the period 1975–2004 were used as a benchmark group. In Section 3, we assessed the evolution of climatic extreme events in the Sahara-Sahel-Arabian Peninsula zone with and without MCB implementation by comparing these three scenarios (Historical, RCP4.5, G4cdnc).

2.4 Climate extreme indices

Owing to length limitations of our research article, it was impossible to analyze all 27 climate indices adopted by the Expert Team on Climate Change Detection and Indices (ETCCDI) (Zhang *et al.*, 2011). Here, we chose six representative climate extreme indices (Table 1): The hottest days (TXx) and the coolest days (TNn) are the extremes of temperature, which we used to assess the intensity of extreme high and low temperature events. The warm spell duration (WSDI) and cold spell duration (CSDI) are the days of temperature above and below a certain threshold, which we used to assess the duration of extreme temperature events. The consecutive dry days (CDD) and the wettest consecutive five days (RX5day) were used to assess the intensity and duration of extreme dry climate events. Each climate extreme index under the three different scenarios [Historical (1975–2004), RCP4.5 (2030–2059) and G4cdnc (2030–2059)] was calculated using the Python library, ICCLIM (Indice Calculation CLIMate).

3. Results and discussion

Although a MCB scheme can act rapidly to mitigate climate change with significant global mean temperature decreases (Stjern *et al.*, 2018), the benefits of MCB are likely to widely vary spatially over the planet, with some regions gaining considerably, whereas others may be faced with a worse set of circumstances than would be the case without MCB (Zhang and Huisingh, 2015). The Sahara-Sahel-Arabian Peninsula zone, as one of the most arid areas on the planet, is sensitive to future climate change. We analyzed six climate extreme indices (Table 1) under three different scenarios (Historical, RCP4.5 and G4cdnc) to understand effects of MCB in mitigating climatic extreme events. Comparing each climate extreme index under RCP4.5 and G4cdnc scenarios, we verified the effects of MCB implementation on mitigating extreme climate change in the Sahara-Sahel-Arabian Peninsula zone. Outputs from simulations under the Historical scenario (1975–2004) were used to compare the extreme climate change between the past and the future.

3.1 Temperature extremes

3.1.1 Hottest days. Under the Historical scenario (1975–2004), the annual TXx index increased significantly only in small parts of the northwestern and central Sahara and the

Downloaded from http://ftp.nowpublishers.com/ijccsm/article-pdf/13/3/250/1144612/ijccsm-06-2020-0051.pdf by guest on 24 May 2026

Category	Index	Description	Definition	Unit
Temperature extremes	TXx	Hottest days	Annual maximum value of daily maximum temperature	°C
	TNn	Coolest days	Annual minimum value of daily maximum temperature	°C
	WSDI	Warm spell duration	Annual count of days with at least six consecutive days when TX > 90th percentile	Days
	CSDI	Cold spell duration	Annual count of days with at least six consecutive days when TN < 10th percentile	Days
Precipitation extremes	CDD	Consecutive dry days	Maximum number of consecutive days when precipitation < 1 mm	Days
	RX5day	Wettest consecutive five days	Maximum of consecutive 5-day (cumulative) precipitation amount	Mm

Table 1.
Definition of climate extreme indices

Notes: TX: maximum temperature; TN: minimum temperature

corresponding trend was 0.2–0.8°C/decade (Figure 1a). Compared with this, under an RCP4.5 emission scenario (2030–2059), the annual TXx index increased significantly in the central and southern Sahara-Sahel zone and the central Arabian Peninsula, with a decadal trend varying from 0.2 to 0.8°C/decade (Figure 1b). Under the implementation of MCB (i.e. G4cdnc scenario) during 2030–2059, the significant increases (0.2–1.0°C/decade) for annual TXx index occurred mainly in Algeria, Morocco and the Sahel belt. Especially, the highest decadal trends (>1.0°C/decade) would occur in the boundary region between Algeria and Tunisia (Figure 1c).

The spatial pattern of the mean annual TXx index was similar under the three climate scenarios (Historical, RCP4.5, G4cdnc). Generally, the Sahara-Sahel-Arabian Peninsula zone had a much larger TXx index than all neighboring regions. The lowest value of mean annual TXx index occurred in the coastal area owing to cooling effects of offshore cold currents. In the central Sahara-Sahel-Arabian Peninsula zone, the mean annual TXx index was about 39–46.5°C during 1975–2004 under the Historical scenario, and it reached 48–51°C during 2030–2059 under RCP4.5 and G4cdnc scenarios. For the coastal area, the mean annual TXx index was still below 36°C for all three scenarios (Figure 1d–f). Without the intervention of MCB, the annual average value of the TXx index in 2030–2059 was predicted to be 2–3°C higher than that in 1975–2004 for most parts of the Sahara and Sahel belt, and the highest increase (2.5–3.5°C) was predicted to occur in the northwestern Sahara and almost the whole Arabian Peninsula (Figure 1g). With the intervention of MCB, the annual average value of TXx index in 2030–2059 was predicted to be 0.5–2°C higher than that in 1975–2004 for the Sahara-Sahel-Arabian Peninsula zone (Figure 1h). Compared with the RCP4.5 scenario, the MCB implementation (G4cdnc scenario) decreased the mean annual TXx index in 2030–2059 by 0.4–1.7°C for the whole Sahara-Sahel-Arabian Peninsula zone, except for Egypt's northern coast (Figure 1i).

3.1.2 Coolest nights. Under the Historical scenario (1975–2004), the annual TNn index demonstrated significantly increased trends only in a negligible fraction of the Sahara with a magnitude of 0.6–1.8°C/decade (Figure 2a). Under scenario RCP4.5, a significantly increased trend during 2030–2059 occurred in about 30% of the Sahel belt, and the trend was about 0–0.9°C/decade (Figure 2b). However, under G4cdnc scenario, no significant trend during 2030–2059 was predicted over almost the whole Sahara-Sahel-Arabian Peninsula zone at the same period (Figure 2c).

Downloaded from http://ftp.nowpublishers.com/ijccsm/article-pdf/13/3/250/1144612/ijccsm-06-2020-0051.pdf by guest on 24 May 2026

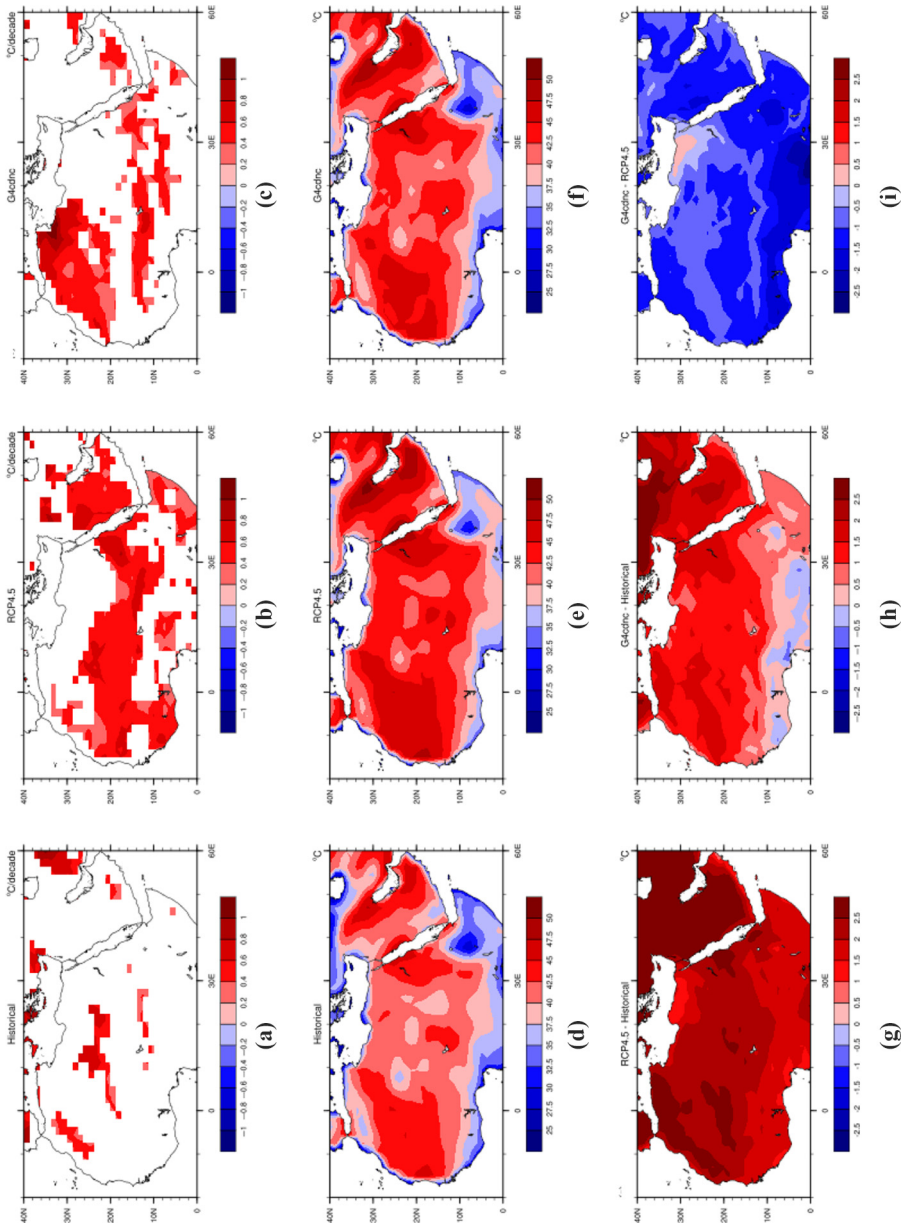

Figure 1. Significant decadal trends of annual TXx index under the three scenarios: (a) Historical (1975–2004), (b) RCP4.5 (2030–2059) and (c) G4cdnc (2030–2059). The spatial patterns of mean annual TXx index under the three scenarios: (d) Historical (1975–2004), (e) RCP4.5 (2030–2059) and (f) G4cdnc (2030–2059). The difference of annual average TXx index between: (g) RCP4.5 and Historical, (h) G4cdnc and Historical and (i) G4cdnc and RCP4.5

Downloaded from http://ftp.nowpublishers.com/ijccsm/article-pdf/13/3/250/1144612/ijccsm-06-2020-0051.pdf by guest on 24 May 2026

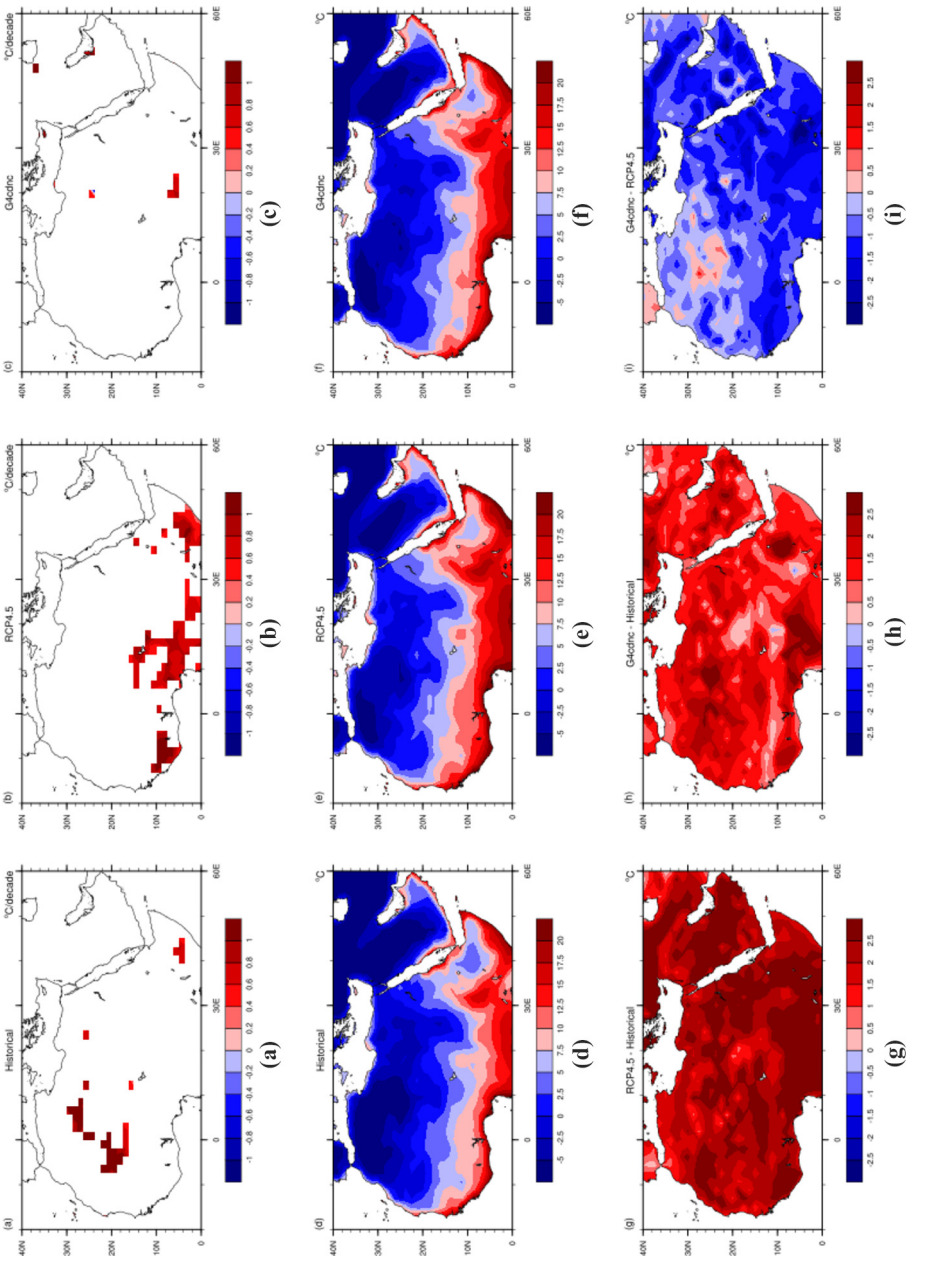

Figure 2.
Significant decadal trends of annual TNn index under the three scenarios: (a) Historical (1975–2004), (b) RCP4.5 (2030–2059) and (c) G4cdnc (2030–2059). The spatial patterns of mean annual TNn index under the three scenarios: (d) Historical (1975–2004), (e) RCP4.5 (2030–2059) and (f) G4cdnc (2030–2059). The difference of average annual TNn index between: (g) RCP4.5 and Historical, (h) G4cdnc and Historical and (i) G4cdnc and RCP4.5

Downloaded from http://ftp.nowpublishers.com/ijccsm/article-pdf/13/3/250/1144612/ijccsm-06-2020-0051.pdf by guest on 24 May 2026

The spatial patterns of the annual TNn index under the three scenarios were similar: the closer to the equator, the higher the annual TNn index. Under the Historical scenario, the lowest annual average TNn index (about −10 to −4°C) during 1975–2004 occurred in the northwestern Sahara and inland in the Arabian Peninsula (Figure 2d). During 2030–2059, no matter whether a MCB scheme was implemented or not, the region where the mean annual TNn index was lower than −5°C was predicted to shrink significantly (Figure 2e,f). When the Historical scenario was compared with the RCP 4.5 scenario, the mean annual TNn index was predicted to increase by more than 1°C in 2030–2059 relative to that in 1975–2004 for the whole Sahara-Sahel-Arabian Peninsula zone, especially with an increase of 2–3°C which occurred in most of Arabian Peninsula (Figure 2g). Comparison of the Historical scenario with the G4cdnc scenario showed that an increase in the mean annual TNn index was controlled at 0–2°C for the whole Sahara-Sahel-Arabian Peninsula zone, except for small regions in the central Sahara (Figure 2h). In summary, in 2030–2059, MCB implementation reduced the mean annual TNn index under an RCP4.5 scenario for most of the Sahara-Sahel-Arabian Peninsula zone by 0.3–2.1°C. But during 2030–2059, in southern Algeria, the average value of TNn index under the G4cdnc scenario was 0.2–0.8°C higher than that under the RCP4.5 scenario. The cooling effect of MCB in the southeastern Sahara-Sahel zone and the whole Arabian Peninsula was greater than in the northwestern Sahara Desert (Figure 2i).

3.1.3 Warm spell duration index. The WSDI index was calculated as annual amount of days with at least six consecutive days when the maximum temperature (TX) exceeded the 90th percentile under the Historical scenario (1975–2004). The trend of the annual WSDI index during 1975–2004 was negligible, only occurring in very limited areas of Arabian Peninsula and the western-northern Sahara Desert with an increasing trend of 7–10 days/decade (Figure 3a). However, under an RCP4.5 scenario, the WSDI index was predicted to have significant increasing trends (13–39 days/decade) over about 90% of the Sahara-Sahel-Arabian Peninsula zone in 2030–2059 (Figure 3b). If a MCB scheme was implemented at the same period, the regions where the trend of annual WSDI index was significant were reduced into the northwestern and eastern Sahara-Sahel zone and most of Arabian Peninsula, and the increasing trend was reduced by about 3 days/decade (Figure 3c).

Under the Historical scenario (1975–2004), the mean annual WSDI index was about 6–12 days over the whole Sahara-Sahel-Arabian Peninsula zone (Figure 3d). However, under the RCP4.5 scenario, the mean annual WSDI index during 2030–2059 reached 43–94 days in Algeria, Libya and Egypt, 91–178 days in southern Sahara Desert, Sahel belt and Arabian Peninsula and about 200 days along the Red Sea coast (Figure 3e). Under the G4cdnc scenario, the mean annual WSDI index over the same period 2030–2059 was predicted to reduce to about 28–57 days in the Sahara-Sahel area, 56–73 days in the Arabian Peninsula and 102 days along the Red Sea coast (Figure 3f). This means that the annual WSDI index under either RCP 4.5 or G4cdnc scenario was predicted to sharply increase from that in 1975–2004 (Figure 3g,h). During 2030–2059, comparing the G4cdnc scenario with the RCP 4.5 scenario, the WSDI index decreased about 7–75 and 118–183 days in the northern part and the southern part of the Sahara-Sahel-Arabian Peninsula zone, respectively (Figure 3i).

3.1.4 Cold spell duration index. The CSDI index was calculated as annual amount of days with at least six consecutive days when night temperature (TN) was below the 10th percentile during 1975–2004 under the Historical scenario. Under the Historical, RCP4.5 and G4cdnc scenarios, no significant trend was revealed for the CSDI index over almost the whole Sahara-Sahel-Arabian Peninsula zone (Figure 4a–c).

Under the Historical scenario (1975–2004), the high mean annual CSDI index occurred over the coastal area and the eastern Sahara and reached 9–13 days (Figure 4d). Under scenario RCP4.5, the mean annual CSDI index during 2030–2059 was reduced to 0 days over

Downloaded from http://ftp.nowpublishers.com/ijccsm/article-pdf/13/3/250/1144612/ijccsm-06-2020-0051.pdf by guest on 24 May 2026

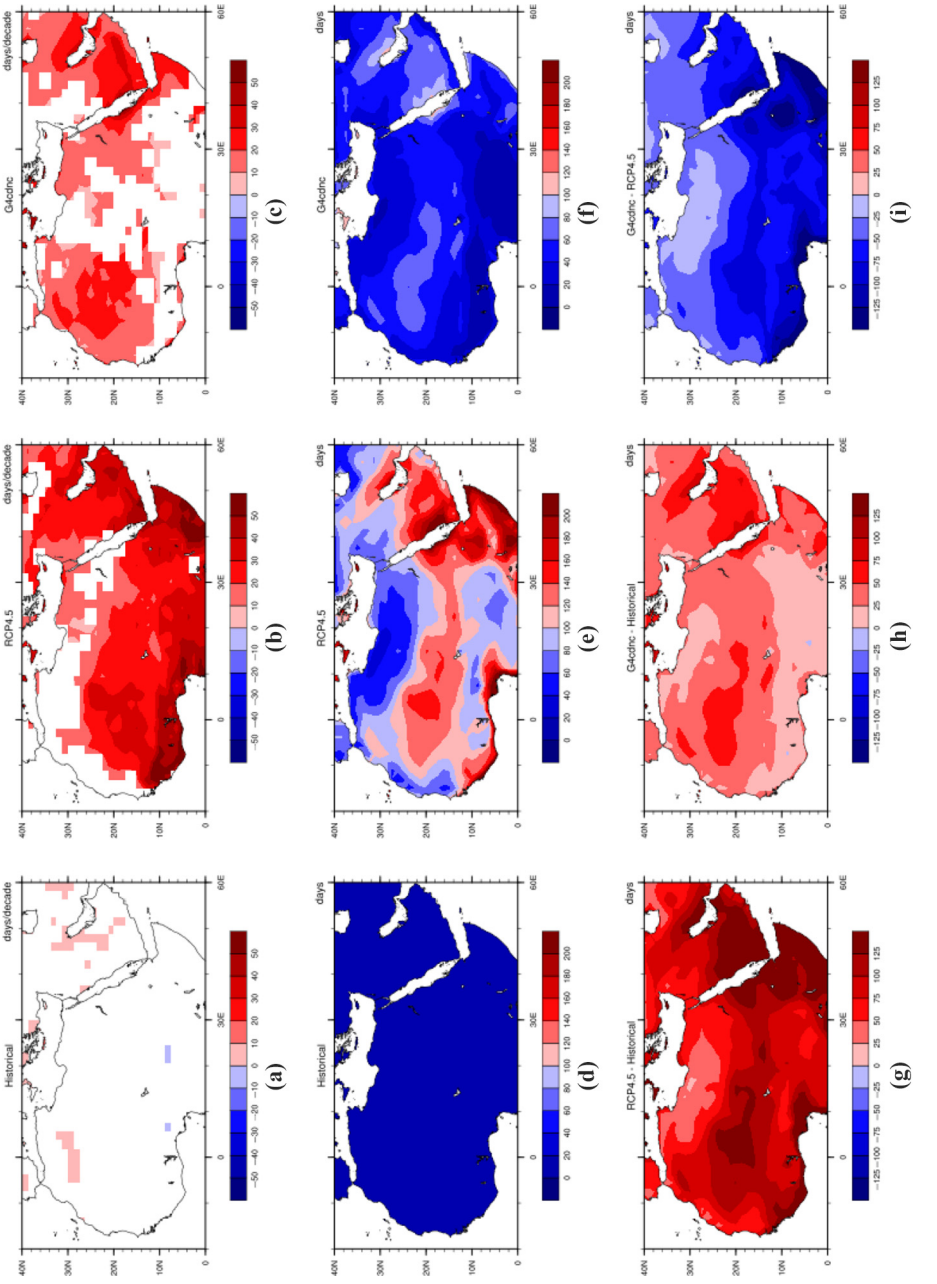

Figure 3.
Significant decadal trends of annual WSDI index under the three scenarios: (a) Historical (1975–2004), (b) RCP4.5 (2030–2059) and (c) G4cdnc (2030–2059). The spatial patterns of mean annual WSDI index under the three scenarios: (d) Historical (1975–2004), (e) RCP4.5 (2030–2059) and (f) G4cdnc (2030–2059). The difference of annual average WSDI index between: (g) RCP4.5 and Historical, (h) G4cdnc and Historical and (i) G4cdnc and RCP4.5

Downloaded from http://ftp.nowpublishers.com/ijccsm/article-pdf/13/3/250/1144612/ijccsm-06-2020-0051.pdf by guest on 24 May 2026

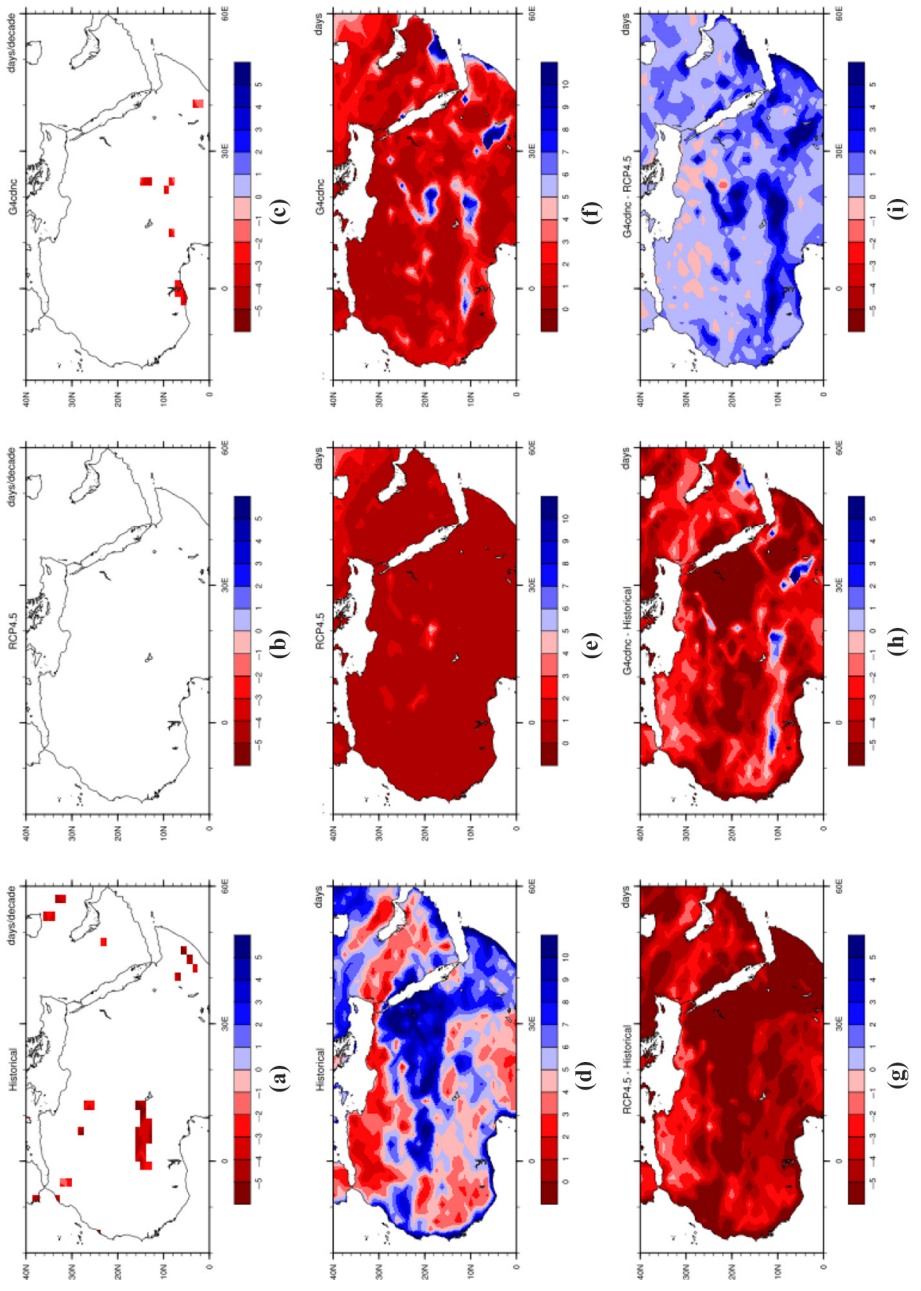

Figure 4.
Significant decadal trends of annual CSDI index under the three scenarios: (a) Historical (1975–2004), (b) RCP4.5 (2030–2059) and (c) G4cdnc (2030–2059). The spatial patterns of mean annual CSDI index under the three scenarios: (d) Historical (1975–2004), (e) RCP4.5 (2030–2059) and (f) G4cdnc (2030–2059). The difference of annual average CSDI index between: (g) RCP4.5 and Historical, (h) G4cdnc and Historical and (i) G4cdnc and RCP4.5

Downloaded from http://ftp.nowpublishers.com/ijccsm/article-pdf/13/3/250/1144612/ijccsm-06-2020-0051.pdf by guest on 24 May 2026

the whole Sahara-Sahel-Arabian Peninsula zone (Figure 4e). However, under the G4cdnc scenario, the mean annual CSDI index during 2030–2059 was predicted to reduce by 4–6 days in the highlands of the Sahara Desert (Figure 4h). Therefore, a MCB scheme could partly alleviate the decrease of the CSDI by 1–3 days over most of the southern Sahara-Sahel-Arabian Peninsula zone, especially 3–8 days in the Sahel belt and the southern coast of the Arabian Peninsula (Figure 4i).

3.2 Precipitation extremes

3.2.1 Consecutive dry days. Under the Historical scenario (1975–2004), the annual CDD index demonstrated a significantly decreased trend only near Lake Chad in Central Sahara, where the trend was 27–53 days/decade (Figure 5a). Under either RCP4.5 or G4cdnc scenarios, there was no significant trend over the whole Sahara-Sahel-Arabian Peninsula zone during 2030–2059 (Figure 5b,c). The spatial patterns of the CDD index were quite similar under all three scenarios (Historical, RCP4.5, G4cdnc): The eastern part of the Sahara Desert had a higher CDD index (253–304 days) than the western part (212–258 days). In the Arabian Peninsula, the higher mean annual CDD index occurred in the southeastern part (257–302 days). However, in the Sahel belt, the mean annual CDD index was about 88–107 days (Figure 5d–f). Although the spatial patterns were similar, the mean annual CDD index under the RCP4.5 scenario during 2030–2059 increased 4–27 days in 1979–2004 in the Sahara Desert and the Arabian Peninsula and decreased 16–21 days in the Sahel belt (Figure 5h). Compared with the RCP4.5 scenario, a MCB scheme decreased the CDD index by 5–25 days over the whole Sahara-Sahel-Arabian Peninsula zone except for the northern Arabian Peninsula, where there was an increase of 14–29 days in the CDD index (Figure 5i).

3.2.2 Wettest consecutive 5 days. A significant trend in the RX5day index under the Historical scenario (1975–2004) only occurred near Lake Chad in Central Sahara, where the trend was 4–23 mm/decade, and no significant trends were found during 2030–2059 under either RCP4.5 or G4cdnc scenarios (Figure 6a-c). The spatial patterns of the RX5day index were also similar under the three climate scenarios (Historical, RCP4.5, G4cdnc), the mean annual RX5day was 3–21 mm over the whole Sahara-Sahel-Arabian Peninsula zone under the Historical scenario (1975–2004), whereas the mean annual RX5day under a RCP4.5 scenario was predicted to decrease by 2–8 mm in the northwestern Sahara in 2030–2059 (Figure 6d,g). It is noteworthy that the RX5day index under the G4cdnc scenario increased by about 10 mm relative to that under the RCP4.5 scenario in the east part of the Sahel belt during 2030–2059 (Figure 6i).

4. Conclusion

As an alternative to direct carbon emissions reduction in industrial and energy sectors, a MCB scheme has been proposed where the increasing radiative forcing caused by anthropogenic carbon emissions is partly offset by an increasing CDNC of low marine clouds. In this study, we focused on the standard G4cdnc scenario, i.e. a MCB scheme was assumed to be implemented through a 50% increase in the CDNC under the RCP4.5 scenario. Owing to the length limitations of our research paper, it was impossible to analyze all 27 climate indices adopted by the ETCCDI (Zhang *et al.*, 2011; Klein Tank *et al.*, 2009). By analyzing six representative climate extreme indices under RCP4.5 and G4cdnc scenarios, we found that a MCB scheme reduced the frequency and intensity of hot wave events and slowed the drought tendency over the whole Sahara-Sahel-Arabian Peninsula zone. It decreased the mean annual TXx index and the TNn index by 0.4-1.7 and 0.3–2.1°C, respectively, for most of the zone, and shortened the WSDI index by 118–183 days and the CSDI index by 1–3 days in the southern zone during 2030–2059. Moreover, it also decreased the mean annual CDD index by 5–25 days over the whole Sahara and Sahel belt, and increased the mean annual RX5day index about 10 mm in the east part of the Sahel belt

Downloaded from http://ftp.nowpublishers.com/ijccsm/article-pdf/13/3/250/1144612/ijccsm-06-2020-0051.pdf by guest on 24 May 2026

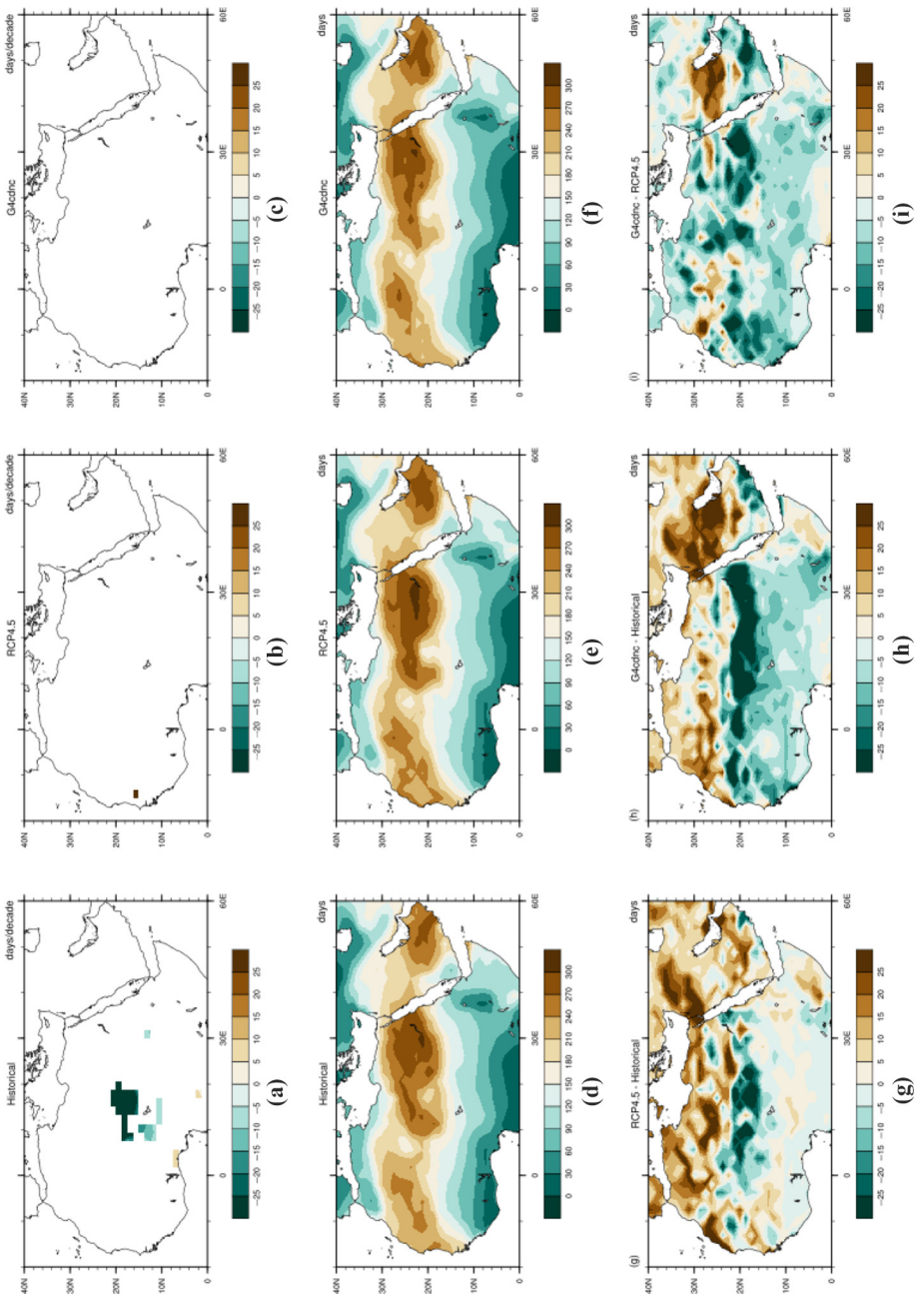

Figure 5.
Significant decadal trends of annual CDD index under the three scenarios: (a) Historical (1975–2004), (b) RCP4.5 (2030–2059) and (c) G4cdnc (2030–2059). The mean annual CDD under the three scenarios: (d) Historical (1975–2004), (e) RCP4.5 (2030–2059) and (f) G4cdnc (2030–2059). The difference of mean annual CDD between: (g) RCP4.5 and Historical, (h) G4cdnc and Historical and (i) G4cdnc and RCP4.5

Downloaded from http://ftp.nowpublishers.com/ijccsm/article-pdf/13/3/250/1144612/ijccsm-06-2020-0051.pdf by guest on 24 May 2026

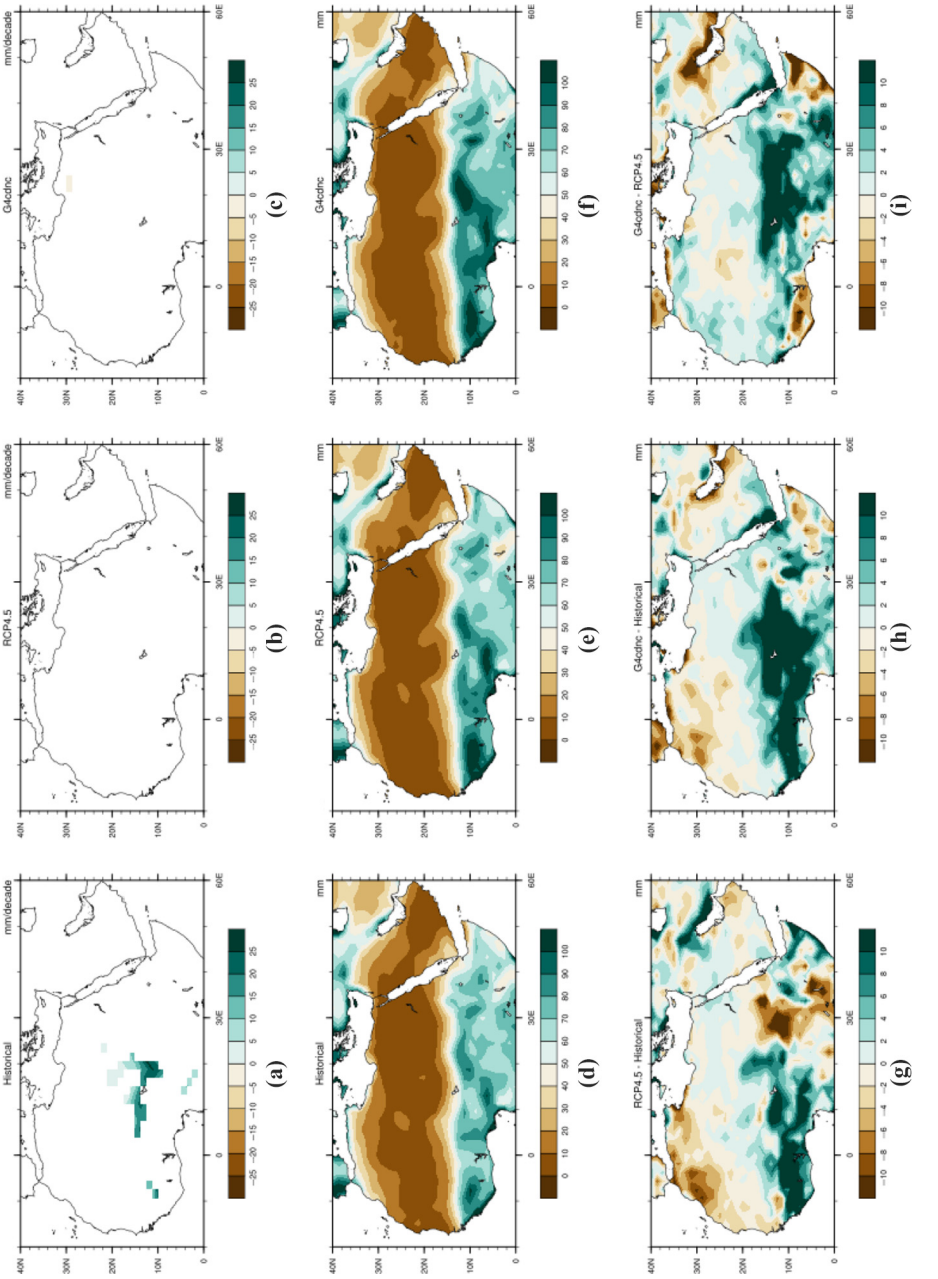

Figure 6.
Significant decadal trends of annual RX5day under the three scenarios: (a) Historical (1975–2004), (b) RCP4.5 (2030–2059) and (c) G4cdnc (2030–2059). Spatial patterns of mean annual RX5day under the three scenarios: (d) Historical (1975–2004), (e) RCP4.5 (2030–2059) and (f) G4cdnc (2030–2059). The difference of mean annual RX5day between: (g) RCP4.5 and Historical, (h) G4cdnc and Historical and (i) G4cdnc and RCP4.5

Downloaded from http://ftp.nowpublishers.com/ijccsm/article-pdf/13/3/250/1144612/ijccsm-06-2020-0051.pdf by guest on 24 May 2026

during 2030–2059. Such mitigation effects on extreme precipitation are very important for the future success of the well-known Great Green Wall project in the Sahel belt, with the aim to prevent the Sahara Desert from expanding southward. At the same time, it is noteworthy that the Sahara-Sahel-Arabian Peninsula zone still tended to be hotter and drier under the G4cdnc scenario in 2030–2059 than in 1975–2004; this means that a 50% increase in the CDNCs of marine clouds is not enough to reverse a future warming trend. At present, severe hot waves in most parts of Sahara-Sahel-Arabian Peninsula zone are already intolerable for human beings, so the Sahara-Sahel-Arabian Peninsula zone will expect to gain considerably from the implementation of MCB owing to mitigating significantly climate extreme events. On the other hand, given the lack of political will to do serious carbon emissions reduction, it appears increasingly likely that the human society will face a future where the alternatives are between catastrophic climate change and MCB scheme. Therefore, it is suggested that policymakers in the Sahara-Sahel-Arabian Peninsula zone consider MCB scheme as a potential emergency shield to catastrophic climate change and resulting disasters.

References

Almagro, A., Oliveira, P.T.S., Rosolem, R., Hagemann, S. and Nobred, C.A. (2020), "Performance evaluation of eta/HadGEM2-ES and eta/MIROC5 precipitation simulations over Brazil", *Atmospheric Research*, Vol. 244, Article No. 105053.

Almazroui, M. (2020), "Summer maximum temperature over the Gulf cooperation council states in the twenty-first century: multimodel simulations overview", *Arabian Journal of Geosciences*, Vol. 13 No. 12, Article No. 477.

Alsarmi, S.H. and Washington, R. (2014), "Changes in climate extremes in the Arabian Peninsula: analysis of daily data", *International Journal of Climatology*, Vol. 34 No. 5, pp. 1329-1345.

Bala, G., Caldeira, K., Nemani, R., Cao, L., Ban-Weiss, G. and Shin, H.J. (2011), "Albedo enhancement of marine clouds to counteract global warming: impacts on the hydrological cycle", *Climate Dynamics*, Vol. 37 Nos 5/6, pp. 915-931.

Brands, S., Herrera, S., Fernandez, J. and Gutierrez, J.M. (2013), "How well do CMIP5 earth system models simulate present climate conditions in Europe and Africa?", *Climate Dynamics*, Vol. 41 Nos 3/4, pp. 803-817.

Caesar, J., Palin, E., Liddicoat, S., Lowe, J., Burke, E., Pardaens, A., Sanderson, M. and Kahana, R. (2013), "Response of the HadGEM2 earth system model to future greenhouse gas emissions pathways to the year 2300", *Journal of Climate*, Vol. 26 No. 10, pp. 3275-3284.

Collins, W.J., Bellouin, N., Doutriaux-Boucher, M., Gedney, N., Halloran, P., Hinton, T., Hughes, J., Jones, C.D., Joshi, M., Liddicoat, S., Martin, G., O'Connor, F., Rae, J., Senior, C., Sitch, S., Totterdell, I., Wiltshire, A. and Woodward, S. (2011), "Development and evaluation of an earth-system model – HadGEM2", *Geoscientific Model Development*, Vol. 4 No. 4, pp. 1051-1075.

Dike, V.N., Shimizu, M.H., Diallo, M., Lin, Z., Nwofor, O.K. and Chineke, T.C. (2015), "Modelling present and future African climate using CMIP5 scenarios in HadGEM2-ES", *International Journal of Climatology*, Vol. 35 No. 8, pp. 1784-1799.

Donat, M.G., Peterson, T.C., Brunet, M., King, A.D., Almazroui, M., Kolli, R.K., Boucherf, D., Al-Mulla, A.Y., Nour, A.Y., Aly, A.A. and Nada, T.A.A. (2014), "Changes in extreme temperature and precipitation in the Arab region: long-term trends and variability related to ENSO and NAO", *International Journal of Climatology*, Vol. 34 No. 3, pp. 581-592.

Griffiths, I.L. (2013), *The Atlas of African Affairs*, Routledge.

Haywood, J.M., Jones, A. and Jones, G.S. (2014), "The impact of volcanic eruptions in the period 2000–2013 on global mean temperature trends evaluated in the HadGEM2-ES climate model", *Atmospheric Science Letters*, Vol. 15 No. 2, pp. 92-96.

Downloaded from http://ftp.nowpublishers.com/ijccsm/article-pdf/13/3/250/1144612/ijccsm-06-2020-0051.pdf by guest on 24 May 2026

Huang, J.P., Guan, X.D. and Ji, F. (2012), "Enhanced cold-season warming in semi-arid regions", *Atmospheric Chemistry and Physics*, Vol. 12 No. 12, pp. 5391-5398.

Johns, T.C., Durman, C.F., Banks, H.T., Roberts, M.J., McLaren, A.J., Ridley, J.K., Senior, C.A., Williams, K.D., Jones, A., Rickard, G.J., Cusack, S., Ingram, W.J., Crucifiifix, M., Sexton, D.M.H., Joshi, M.M., Dong, B.-W., Spencer, H., Hill, R.S.R., Gregory, J.M., Keen, A.B., Pardaens, A.K., Lowe, J.A., BodasSalcedo, A., Stark, S. and Searl, Y. (2006), "The new Hadley Centre climate model HadGEM1: evaluation of coupled simulations", *Journal of Climate*, Vol. 19 No. 7, pp. 1327-1353.

Jones, A., Haywood, J. and Boucher, O. (2009), "Climate impacts of geoengineering marine stratocumulus clouds", *Journal of Geophysical Research: Atmospheres*, Vol. 114, Article ID: D10106.

Jones, C.D., Hughes, J.K., Bellouin, N. and Hardiman, S.C. (2011), "The HadGEM2-ES implementation of CMIP5 centennial simulations", *Geoscientific Model Development*, Vol. 4 No. 3, pp. 543-570.

Kravitz, B., Caldeira, K., Boucher, O., Robock, A., Rasch, P.J., Alterskjær, K., Karam, D.B., Cole, J.N., Curry, C.L., Haywood, J.M. and Irvine, P.J. (2013a), "Climate model response from the geoengineering model intercomparison project (GeoMIP)", *Journal of Geophysical Research: Atmospheres*, Vol. 118 No. 15, pp. 8320-8332.

Kravitz, B., Forster, P.M., Jones, A., Robock, A., Alterskjær, K., Boucher, O., Jenkins, A.K., Korhonen, H., Kristjánsson, J.E., Muri, H. and Niemeier, U. (2013b), "Sea spray geoengineering experiments in the geoengineering model intercomparison project (GeoMIP): experimental design and preliminary results", *Journal of Geophysical Research: Atmospheres*, Vol. 118 No. 19, pp. 11-175.

Meinshausen, M., Smith, S.J., Calvin, K., Daniel, J.S., Kainuma, M.L.T., Lamarque, J.F., Matsumoto, K., Montzka, S.A., Raper, S.C.B., Riahi, K. and Thomson, A.G.J.M.V. (2011), "The RCP greenhouse gas concentrations and their extensions from 1765 to 2300", *Climatic Change*, Vol. 109 Nos 1/2, p. 213.

Moss, R.H., Edmonds, J.A., Hibbard, K.A., Manning, M.R., Rose, S.K., van Vuuren, D.P., Carter, T. R., Emori, S., Kainuma, M., Kram, T., Meehl, G.A., Mitchell, J.F.B., Nakicenovic, N., Riahi, K., Smith, S.J., Stouffer, R.J., Thomson, A.M., Weyant, J.P. and Wilbanks, T.J. (2010), "The next generation of scenarios for climate change research and assessment", *Nature*, Vol. 463 No. 7282, pp. 747-756.

Ragab, R. and Prudhomme, C. (2002), "SW – soil and water: climate change and water resources management in arid and semi-arid regions: prospective and challenges for the 21st century", *Biosystems Engineering*, Vol. 81 No. 1, pp. 3-34.

Shiru, M.S., Shahid, S., Dewan, A., Chung, E.S. and Hassan, Q.K. (2020), "Projection of meteorological droughts in Nigeria during growing seasons under climate change scenarios", *Scientific Reports*, Vol. 10 No. 1, Article ID: 10107.

Stjern, C.W., Muri, H., Ahlm, L., Boucher, O., Cole, J.N., Ji, D., Jones, A., Haywood, J., Kravitz, B., Lenton, A. and Moore, J.C. (2018), "Response to marine cloud brightening in a multi-model ensemble", *Atmospheric Chemistry and Physics*, Vol. 18 No. 2, pp. 621-634.

Tarawneh, Q.Y. and Faraj, T.K. (2020), "The effect of anthropogenic activity on the extreme climate events and solar irradiation in Saudi Arabia", *Arabian Journal of Geosciences*, Vol. 13 No. 14, Article ID. 616.

Taylor, K.E., Stouffer, R.J. and Meehl, G.A. (2012), "An overview of CMIP5 and the experiment design", *Bulletin of the American Meteorological Society*, Vol. 93 No. 4, pp. 485-498.

Zhang, Z. and Huisingh, D. (2015), "Review of geoengineering approaches to mitigating climate change", *Journal of Cleaner Production*, Vol. 103, pp. 898-907.

Zhang, Q., Xu, C.Y., Zhang, Z.X. and Chen, Y.D. (2009), "Changes of temperature extremes for 1960-2004 in far-west China", *Stochastic Environmental Research and Risk Assessment*, Vol. 23 No. 6, pp. 721-735.

Zhang, X., Alexander, L., Hegerl, G., Jones, P., Klein, T.A., Peterson, T.C., Trewin, B. and Zwiers, F.W. (2011), "Indices for monitoring changes in extremes based on daily temperature and precipitation data", *Wiley Interdisciplinary Reviews: Climate Change*, Vol. 2 No. 6, pp. 851-870.

Downloaded from http://ftp.nowpublishers.com/ijccsm/article-pdf/13/3/250/1144612/ijccsm-06-2020-0051.pdf by guest on 24 May 2026

About the authors

Yuanzhuo Zhu is a graduate student and an active member of climate modeling laboratory at Shandong University, China.

Zhihua Zhang is Taishan Distinguished Professor and Director of Climate Modeling Laboratory at Shandong University, China. He has published five first-authored books in Elsevier/Springer and published more than 50 first-authored articles. Professor Zhang has served as the Editor-in-Chief of *International Journal of Big Data Mining for Global Warming* (World Scientific), Topical Chief Editor of *Arabian Journal of Geosciences* (Springer), Associate Editor of *Environment, Development and Sustainability* (Springer) and so on. Zhihua Zhang is the corresponding and co-first author and can be contacted at: zhangzhihua@sdu.edu.cn

Professor M. James C. Crabbe is a Supernumerary Fellow at Wolfson College, Oxford University, UK. His research, spanning biomedical and environmental sciences, education and the humanities has resulted in 276 research publications in refereed journals, books, book chapters and reviews, plus 14 items of commercial molecular modeling software. In 2018, he won the Annual Scientific Award of the International Engineering and Technology Institute (IETI), and in 2006 he won the 6th Aviva/Earthwatch International Award for Climate Change Research. In 2008, he received the Award of Outstanding International Contribution to the Creative Industry of China during the 3rd China Creative Industry Awards, presented at the Diaoyutai State Guesthouse in Beijing.

For instructions on how to order reprints of this article, please visit our website:
www.emeraldgrouppublishing.com/licensing/reprints.htm
Or contact us for further details: **permissions@emeraldinsight.com**

Downloaded from http://ftp.nowpublishers.com/ijccsm/article-pdf/13/3/250/1144612/ijccsm-06-2020-0051.pdf by guest on 24 May 2026